Environmental Science & Technology

Article

pubs.acs.org/est

A Scenario and Forecast Model for Gulf of Mexico Hypoxic Area and Volume

Donald Scavia,*[,†,‡] Mary Anne Evans,[§] and Daniel R. Obenour[‡]

[†]Graham Sustainability Institute, University of Michigan, Ann Arbor, Michigan 48104, United States

[‡]School of Natural Resources and Environment, University of Michigan, Ann Arbor, Michigan 48109, United States

[§]U.S. Geological Survey Great Lakes Science Center, Ann Arbor, Michigan 48105, United States

ABSTRACT: For almost three decades, the relative size of the hypoxic region on the Louisiana-Texas continental shelf has drawn scientific and policy attention. During that time, both simple and complex models have been used to explore hypoxia dynamics and to provide management guidance relating the size of the hypoxic zone to key drivers. Throughout much of that development, analyses had to accommodate an apparent change in hypoxic sensitivity to loads and often cull observations due to anomalous meteorological conditions. Here, we describe an adaptation of our earlier, simple biophysical model, calibrated to revised hypoxic area estimates and new hypoxic volume estimates through Bayesian estimation. This application eliminates the need to cull observations and provides revised hypoxic extent estimates with uncertainties corresponding to different nutrient loading reduction scenarios. We compare guidance from this model application, suggesting an approximately 62% nutrient loading reduction is required to reduce Gulf hypoxia to the Action Plan goal of 5000 km^2, to that of previous applications. In addition, we describe for the first time, the corresponding response of hypoxic volume. We also analyze model results to test for increasing system sensitivity to hypoxia formation, but find no strong evidence of such change.

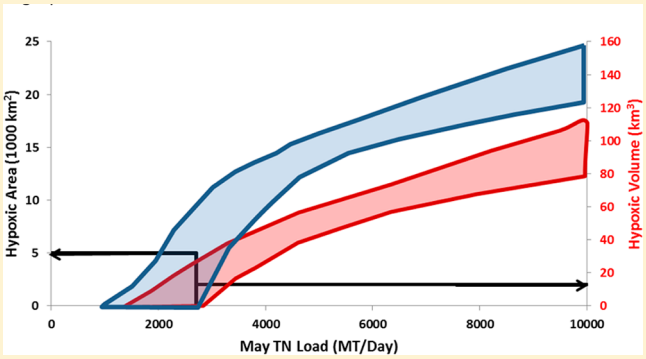

INTRODUCTION

For almost three decades, the relative size of the hypoxic region on the Louisiana-Texas continental shelf has drawn scientific and policy attention.[1−8] During that time, several models, from simple regressions[9−13] to more complex biophysical models,[14−16] have been used to explore hypoxia dynamics and provide management guidance relating the size of the hypoxic zone to key drivers that can be controlled, such as nutrient loads.[17−20]

During the course of that development several efforts, including our own, explored what was believed to be a change in the sensitivity of hypoxic area to nutrient loads based on, for example, changes in the ratio of hypoxia area to load and alterations in biophysical model parameters required to improve model fit.[12,13,21,22] These analyses were based primarily on the apparent fact that hypoxic area increased over the time period of analysis, whereas the nitrogen load had not. However, a recent reassessment of the time course of hypoxic area, based on statistically rigorous geospatial estimation methods,[23] showed that those increases in hypoxic area were, at least in part, artifacts of sampling design and interpolation limitations, and that change in hypoxic area over the last few decades was likely less than previously thought. That work did indicate, however, that hypoxic volume may have increased more than hypoxic area.

Several simulation and forecast models developed during this time period also culled the observation suite,[10,11] or otherwise tried to avoid,[20,21] "outliers" associated with hurricanes and strong tropical storms, because when those events occur near the time of shelfwide hypoxia surveys they tend to mix the water column and create smaller hypoxic areas. Other conditions, such as the presence of relatively strong currents from the west "piling up" hypoxic waters and reducing measures of areal extent,[3,10] have also confounded models.

These three issues—apparent changes in sensitivity, impacts of storms, and strong current reversals—have until now made development of a temporally consistent and policy-relevant model difficult. Herein, we describe an adaptation of our earlier, simple biophysical model,[17−21] calibrated to the revised area estimates and the new volume estimates[23] through Bayesian estimation. This model eliminates the need to cull observations, allows another test on changes in system sensitivity, and provides revised scenario predictions and forecasts with uncertainties. We compare guidance from this model to that made earlier for setting target loads to reduce Gulf hypoxia to the Action Plan goal of 5000 km^2.

Received: June 7, 2013
Revised: August 14, 2013
Accepted: August 20, 2013
Published: August 20, 2013

   dx.doi.org/10.1021/es4025035 | *Environ. Sci. Technol.* 2013, 47, 10423−10428

MATERIALS AND METHODS

Data. May total nitrogen (TN) loading,[24] computed as the sum of Kjeldahl nitrogen, NO_2, and NO_3, for the Mississippi (at St. Francisville, MS) and Atchafalaya rivers (at Melville, LA) was the primary model driver. Hypoxic area and volume estimates and their uncertainties were based on a reassessment[23] of the 1985−2011 annual shelf-wide cruise data of the Louisiana University Marine Consortium.[2]

Model. The model is the same as that developed originally to relate Gulf of Mexico hypoxic area to loads from the Mississippi and Atchafalaya rivers.[17] It has subsequently been used in comparison to other models,[18] for exploring nitrogen vs phosphorus control,[19] to provide guidance for the 2001 and 2008 Gulf Action Plans,[6,7] and to explore potential impacts of climate-induced changes in nutrient delivery.[25] It is an adaptation of the Streeter-Phelps river model that simulates oxygen concentration downstream from point sources of organic matter loads based on mass balance equations for oxygen-consuming organic matter, in oxygen equivalents (i.e., biochemical oxygen demand, BOD), and dissolved oxygen concentration (DO). Assuming no upstream oxygen deficit, and ignoring longitudinal dispersion, the model's steady state solution for DO is:

for $x < 220$ km

$$DO_y(x) = DO_s - \left(\frac{k_d BOD_{m,y}}{k_r - k_d}\right)\left(e^{(-k_d x/v)} - e^{(-k_r x/v)}\right)$$

for $x \geq 220$ km

$$DO_y(x) = DO_s - \left(\frac{k_d BOD_{m,y}}{k_r - k_d}\right)\left(e^{(-k_d x/v)} - e^{(-k_r x/v)}\right) - \left(\frac{k_d BOD_{a,y}}{k_r - k_d}\right)\left(e^{(-k_d (x-220)/v)} - e^{(-k_r (x-220)/v)}\right)$$

Where y = year index, x = distance from the Mississippi River mouth (km), DO = DO (mg L^{-1}), DO_s = DO saturation concentration (mg L^{-1}), k_d = first order organic matter decay rate (d^{-1}), k_r = first order reaeration rate of the lower layer (d^{-1}), and BOD = BOD load for the Mississippi (m) and Atchafalaya (a) rivers (where the Atchafalaya River enters 220 km west of the Mississippi River). In the original Streeter-Phelps model for rivers, v represents the downstream velocity in km d^{-1}. However, in this application, its interpretation is more complicated because it is a bulk calibration parameter that represents a combination of the net effect of surface and bottom layer flow and sinking of organic matter into the bottom layer.

Organic matter load and associated BOD was approximated by multiplying TN loads by the Redfield ratio to convert nitrogen to algal carbon (5.67 $gCgN^{-1}$), and by assuming an oxygen equivalent (e.g., respiratory ratio) of 3.47 gO_2gC^{-1}. We assumed 50% of the Mississippi River load moved east or offshore and did not contribute to hypoxia development,[26] and that all of the surface algal production settled below the pycnocline.

The model produces a subpycnocline DO concentration profile stretching from the mouth of the Mississippi River toward the Louisiana-Texas border. From that profile, we determined the total length for which DO < 3 mg L^{-1}. A value of 3 mg L^{-1} was used because that average subpycnocline DO concentration roughly corresponds in time to a bottom water DO concentration of 2 mg L^{-1} and hypoxic conditions.[17] Hypoxic length is then converted to area ($area_y$) using an empirical formula determined from geospatial model output: $area_y = 57.8 \text{ length}_y$. Hypoxic volume ($vol_y$), when modeled, is determined as $vol_y = area_y \times \tau_1 + area_y^2 \times \tau_2$, where τ_1 and τ_2 are empirical model parameters. This nonlinear relationship between volume and area represents the fact that hypoxic thickness tends to increase with increasing hypoxic area.[23]

Bayesian Calibration. Calibration was conducted using Markov Chain Monte Carlo (MCMC) implementation of Bayes Theorem using WinBUGS (version 1.4.3) called from R (version 2.6.0, R2WinBUGS, version 2.1-8). The use of Bayesian calibration allows all parameters to be represented as probability distributions, thus ensuring propagation and quantification of uncertainty. The calibrated joint posterior parameter distribution reflects the prior parameter distributions (described below) updated by the joint maximum likelihood parameter distribution (reflecting a least-squares fit to the calibration data set).[27] All calibrations were run until full mixing was achieved between three independent MCMC chains, indicating convergence on the posterior parameter distribution. Mixing was monitored using the ratio of among chain to within chain variance ($\hat{r}$), and chains were considered mixed when $\hat{r} < 1.1$ for all parameters.[27]

Unless otherwise noted, the following constants and prior-distributions were used: $DO_s = 7$ (consistent with surface layer observations), $k_r = 0.1$,[28] $k_d \sim U(0.001,0.01)$, $v \sim U(0, 10)$, $\tau_1 \sim N(5,3.2)I(0,)$, and $\tau_2 \sim N(5,3.2)I(0,)$ where N and U represent normal and uniform distributions, respectively. The numbers in the first parentheses are the mean and standard deviation (SD) for normal distributions or lower and upper bounds for uniform distributions, and I(#,#) indicates truncation at the values in the parentheses.

Uncertainty in model predictions was accounted for based on the following relationships:

$$area_y \sim N(area_{predict,y}, \sigma^2_{area})$$

$$vol_y \sim N(vol_{predict,y}, \sigma^2_{vol})$$

Similarly, uncertainty in the geostatistical (geo) model estimates[23] was accounted for using:

$$area_{geo,y} \sim N(area_y, \sigma^2_{geo,y})$$

$$vol_{geo,y} \sim N(vol_y, \sigma^2_{geo,y})$$

In these equations, $area_y$ and vol_y can be thought of as the true (but unknown) extent distributions, which are only considered internally within the model.[29]

Model Comparison. We explored three models without excluding any years: (1) model of hypoxic area, allowing v to vary by year, (2) model of hypoxic area, with all parameters held constant across all years, and (3) model of hypoxic area and volume allowing v, k_r, and τ_1 to vary based on approximated weather affects. For cases 1 and 2, the priors were used as described above, except that v was estimated for each year in case 1.

Case 3 explored explicitly weather impacts on hypoxic area and volume. We categorized 1998 and 2009 as years with unusually strong westerly winds in the two month period preceding the shelfwide cruise ("wind years"). The westerly wind velocities for these years were 0.96 and 1.11 m/s, respectively, compared to a mean of −0.44 m/s. We categorized 1988, 1989, 1997, and 2003 as "storm years" because they met two criteria: (1) according to NOAA storm track data, there were tropical storms or hurricanes in the vicinity of the study area within two weeks of the beginning of the shelfwide cruise and (2) based on coastal weather stations,

wind stresses (wind speed squared) were unusually high in the two weeks leading up to the shelfwide cruises (>35 m^2/s^2). The wind velocity and wind stress data used in this analysis are averages from stations at Sabine Pass and Southwest Pass, with missing data supplemented from Calcasieu Pass and Grand Isle, respectively.[30]

For "wind years", the flow-dependent ν was fit with a prior $\nu_w \sim U(0, 10)$ and τ_{1w} was fit with the prior $\tau_{1w} \sim N(5,3.2)I(0,)$. For "storm years", the reaeration term (k_r) was fit with a prior of $k_{r,w} \sim U(0, 0.5)$. All other parameter values were held constant across categories with the priors or values given above.

Rate Calculations. Profiles of subpycnocline water column respiration were calculated as the product of k_d and the concentration of BOD. Means and SDs were calculated across years for each model segment, and spatial average and SD values were then calculated across model segments corresponding to the spatial ranges of available comparison studies.

RESULTS AND DISCUSSION

As in the original model application,[17] the overparameterized calibration allowing ν to vary by year (case 1) explained most of the interannual variability of area (area R^2 = 1.00, Table 1);

Table 1. Parameter Estimates for Case 1, With Values of ν Allowed Varying Each Year and All Other Parameters Constant

	mean	SD	2.5%	97.5%
k_d	0.091	0.008	0.071	0.100
σ^2_{area}	2.78	2.74	0.11	9.43

however, in contrast to earlier applications using the uncorrected hypoxic area data set,[17,20,21] ν showed considerable variability but little pattern with time (Figure 1). The wind and storm years

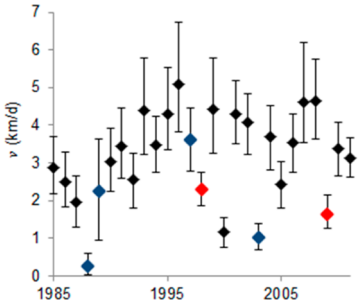

Figure 1. Case 1 estimates of ν. Black symbols are normal years, blue are storm years, and red are wind years.

tended to be among the lower ν's. This case demonstrates the ability of the model formulation to fit the observations closely, if ν is known. However, because ν represents an unknown combination of physical conditions, a model specifying ν for each year is of little predictive value. In earlier applications,[17,25] ν for prediction purposes was drawn from the distribution of annual ν's, holding all other parameters constant, in Monte Carlo simulations. Here, in cases 2 and 3, we treat it as one of the values to be estimated in the Bayesian application.

Fitting all parameters as constants across all years (case 2) produced a moderate fit to hypoxic area (R^2 = 0.50) with parameters falling within ranges estimated in previous applications (Table 2). This model fit was slightly better than in the original application (R^2 = 0.45), which covered a smaller

Table 2. Parameter Estimates for Case 2 with All Parameters Held Constant

	mean	SD	2.5%	97.5%
ν	2.16	0.31	1.80	3.05
k_d	0.03	0.02	0.02	0.08
σ^2_{area}	4.43	0.76	3.20	6.12

study period and was calibrated to an earlier version of hypoxic area estimates.[17] We tested model residuals for a trend with time by developing a simple linear regression of residuals as a function of time (year), accounting for model and observation uncertainty. Our analysis does not indicate a significant trend (slope = 42 ± 131 [±standard error] km^2/yr) as the 90% credible interval includes zero (i.e., the slope coefficient is less than 1.65 standard errors from zero). Thus, the case 2 results provide no strong evidence for the changes in system sensitivity that have been suggested by earlier studies.[12,13,21,22]

Table 3. Parameter Estimates for Case 3, With Weather Categories for ν, τ_1, and k_r

	mean	SD	2.5%	97.5%
ν normal years	2.25	0.22	1.99	2.83
ν wind years	1.09	0.25	0.67	1.61
τ_1 normal years	2.05	1.01	0.18	3.87
τ_1 wind years	4.94	1.79	1.69	8.73
τ_2	0.11	0.06	0.01	0.23
k_d	0.026	0.010	0.017	0.050
k_r storm years	0.15	0.03	0.11	0.20
σ^2_{area}	3.07	0.69	1.90	4.56
σ^2_{vol}	13.81	4.04	7.03	22.94

The case 3 model (Table 3, Figure 2) that uses weather categories is a better fit to the observations, with 69% of the interannual variability in area and 61% of the interannual variability in volume explained. An analysis of residuals (Figure 3) hints at an upward trend in hypoxic volume, but for neither area nor volume are the trends statistically significant (slope = 75 ± 100 km^2/yr for area and 0.72 ± 0.50 km^3/yr for volume).

The critical new feature of case 3 was to allow the coefficient, ν, to take on a different value in years when there were strong westerly winds (Table 3). The resulting difference (2.24 in normal years; 1.09 in strong westerly wind years) is expected because ν includes the effect of currents and one would expect westerly winds to impede westward flow. The resulting estimates of hypoxic thickness (combined effect of τ_1 and τ_2) were also consistent with strong westerly winds generating thicker layers (τ_{1w} = 4.94) compared to normal years (τ_1 = 2.05). Allowing the mixing term, k_r, to take on different values during storm years, resulted in a mixing rate slightly higher (0.15 vs 0.1) than for nonstorm years. The primary advantage of case 3 over earlier applications[18,21] is that it accounts for the variability of all years (i.e., no outliers) and model performance is substantially improved over the version with constant parameters (case 2). Rather than dropping the 12 observations from the six outlier years, we add only three parameters (ν and τ_1 for "wind years" and k_r for "storm years"). In addition, in doing so, the altered parameter estimates are consistent with expected physical changes. Because of these benefits, we focus on case 3 throughout the remainder of this discussion.

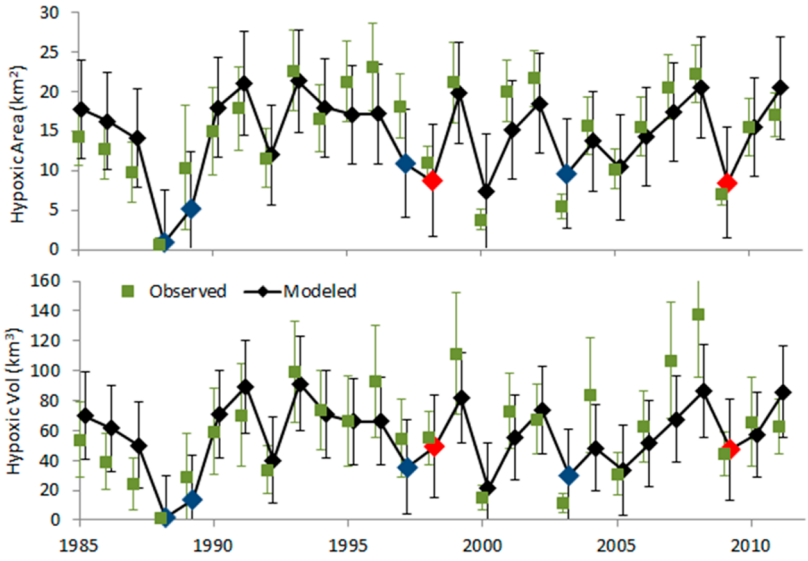

Figure 2. Modeled (diamonds) and observed (boxes) hypoxic area (top) and volume (bottom) for case 3 with 95% CI as error bars. Black diamonds represent model output for normal years, blue diamonds for storm years, and red diamonds for wind years.

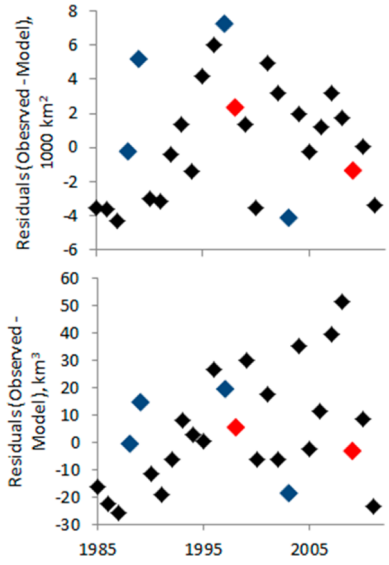

Figure 3. Case 3 model residuals for hypoxic area (top) and volume (bottom). Black symbols are normal years, blue are storm years, and red are wind years.

When comparing modeled rates of subpycnocline oxygen consumption from earlier applications[17,21] to observations, modeled rates fell within the rather broad range of observations available at the time. However, Murrell et al.[31] recently pointed out that those modeled rates fall considerably outside the range of their more recent and more comprehensive measurements. Therefore, we compare the results from this version of the model with those estimates (Figure 4), as well as to those from another recent set of observations that include both water column and sediment oxygen consumption rates.[32] Given the variability associated with the observations and the rather simple biophysical abstraction of the model, modeled rates are reasonably consistent with the two sets of measurements. This difference from our earlier applications[20,21] is a result of different estimates of k_r.

Murrell et al.[31] reported bottom-layer and mid-depth water column respiration across the entire hypoxic shelf region throughout spring and summer 2003−2007. The mean and SD of their observations for March−August are 0.24 ± 0.023 and 0.26 ± 0.080 mg/L/day, respectively (from their Table 2). Assuming, as they did, that sediment demand is approximately 20% of water column demand (also consistent with McCarthy et al.[32]), the means would approach 0.29 and 0.32 mg/L/day. For comparison to those measurements, our corresponding subpycnocline rates and SD are 0.5 ± 0.3, averaged over the model domain of 50−400 km from the mouth of the Mississippi River. In another study, McCarthy et al.[32] measured subpycnocline respiration and sediment oxygen demand during spring and summer 2008−2011, primarily on the eastern portion of the shelf. Using their areal rates, their estimates of corresponding subpycnocline thickness, their average sediment demand of 0.073 mg/L/day for cases when it was not measured, and omitting the September 2008 station they describe as significantly influenced by hurricanes, we calculate rates of 0.65 ± 0.26 mg/L/day averaged over May−September. For comparison to those measurements, our corresponding rates and SD are 0.44 ± 0.29 for all years, averaged over the model domain from 70 to 225 km from the mouth of the Mississippi River. The model profile, with high respiration rates near the mouths of the Mississippi and Atchafalaya rivers (Figure 4), is a consequence of the simplifying assumption that those loads are treated as point sources of BOD at the discharge points.

Because the Action Plan goal is based on a 5-year running average and because "storm" and "wind" years are often absent for extended periods (e.g., 1990−1996 and 2004−2008), response curves and credible intervals for management scenarios (Figure 5) are based on case 3 parameters for "normal" years. However, for annual forecasting purposes, where the future weather condition is unknown, the forecast and credible interval are based on sampling from the case 3 parameters for all weather conditions (normal, wind, and storm years) at the proportion of the years these different weather conditions have occurred throughout the study period. As one would expect, the forecasting credible intervals assuming unknown weather are relatively wide. (It may be possible to update forecasts a week or two prior to the monitoring cruise when weather conditions become more clear.)

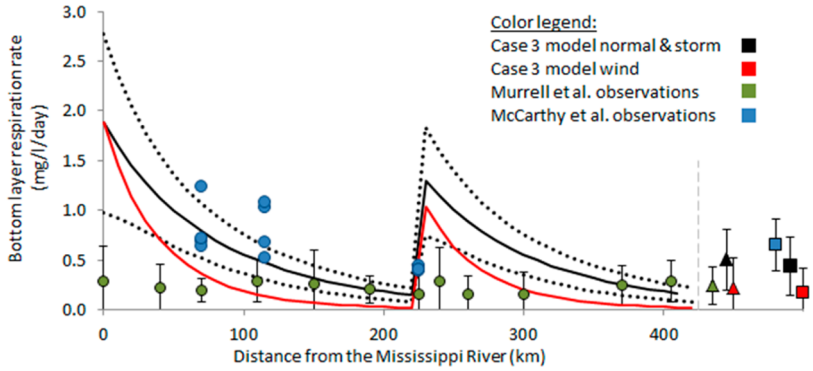

Figure 4. Comparison of modeled and measured subpycnocline respiration rates. Case 3 modeled respiration for different weather categories as solid (black and red) lines. SD of modeled normal (& storm) respiration as dotted black lines (here, the SD reflects yearly loading variability and model uncertainty). Green circles are from Figure 4 in Murrell et al.[31] with error bars representing SD (calculated from their standard error and number of samples). Blue circles are from McCarthy et al.[32] Triangular symbols represent March−August mean and SD from Table 2 in Murrell et al.[31] and model output averaged over the spatial domain corresponding to the Murrell et al. Square symbols represent the cruise mean and SD from McCarthy et al. (blue box), and model output averaged over the spatial domain corresponding to McCarthy et al.

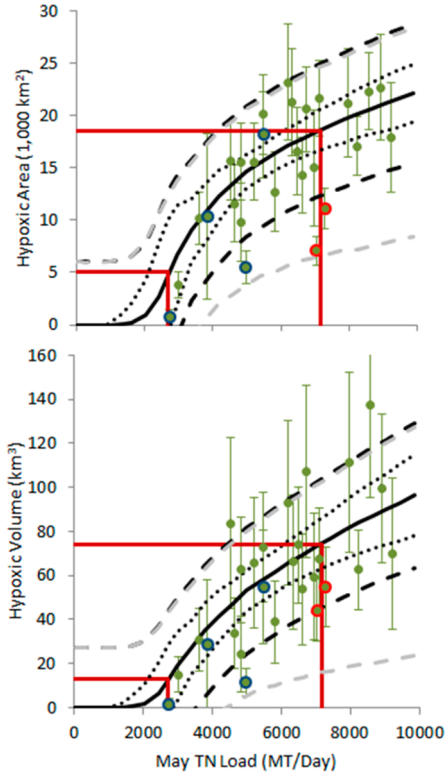

Figure 5. Case 3 response curves for hypoxic area (top) and volume (bottom) as a function of May TN load. Observed areas and volumes are shown as green circles with 95% CI; circles with blue outlines denote storm years and red outlines denote wind years. The best estimate curve for normal years is represented by the black solid line. The 95% CI for the mean response of normal years is represented by dotted black lines. The 95% CI for individual annual responses (i.e., the forecast uncertainty) is represented as dashed black lines assuming normal weather, and as dashed gray lines for unknown weather. Red vertical and horizontal lines represent the 2007−2011 average May TN Load and the load required to achieve a 5,000 km^2 hypoxic area.

These results (Figure 5) indicate that to reach the 5-year running average Action Plan goal of 5000 km^2 (i.e., a 70% reduction from the 2007−2011 mean hypoxic area), the May TN load would have to be reduced by 62% (54−71% CI) from the 2007−2011 average of 7160 MT/day. Recommendations in the past have suggested reducing the annual TN load by 45−55% from the 1980−1996 average.[8] The new recommendation of 62% reduction is consistent with that range, recognizing that the 2007−2011 May TN load is roughly 10% higher than the 1980−1996 average load. It is also interesting to note that we project the 62% reduction in May TN load will result in an approximately 84% reduction in hypoxic volume relative to 2007−2011 conditions (83 km^3 reduced to 13 km^3).

This modeling application was calibrated to new hypoxic extent estimates, as determined from a recent study using statistically rigorous geospatial estimation methods.[23] As such, this is an important update to earlier hypoxia modeling studies based on previous hypoxic area estimates.[10,11,13,17,19−22] However, this update does not alter the requirement that substantial loading reductions are needed to reach the Action Plan goal of a 5000 km^2 (or less) average hypoxic area. Our upward estimate of 62% reflects the fact that loads have increased since the original Action Plan. In its review of the original hypoxia assessment and subsequent work, the EPA Science Advisory Board[8] noted in 2007 that the scientific basis for the need to reduce the loads has become stronger while actions to implement those reductions have lagged, and the U.S. Geological Survey[33] reported that little consistent progress had been made in reducing riverine nitrate concentrations in the Mississippi River and its tributaries since 1980, and that conditions are worsening in some areas.

Another implication of our work is that hypoxic volume appears to respond more dramatically to loading reductions than does hypoxic area (i.e., 84% vs 70% reduction for the same load reduction). This is because the thickness of the hypoxic zone tends to increase with increasing area, as shown by Obenour et al.[23] and reflected in the parameter τ_2 of our model. Finally, we demonstrated that by careful addition of a small number of "special-case" parameters, related to years with unusual weather conditions, we were able to develop a model that considers, as opposed to removes, years dismissed as outliers in earlier applications.

This adaptation of the Streeter-Phelps river model has been used extensively for the Gulf of Mexico, where the strong coastal current has been parametrized as a westward flowing stream. It has also been applied successfully to the Chesapeake Bay,[34,35] and could be a relevant option for modeling most drowned river

dx.doi.org/10.1021/es4025035 | Environ. Sci. Technol. 2013, 47, 10423−10428

mouth estuaries or systems that can be approximated as fundamentally one-dimensional.

AUTHOR INFORMATION

Corresponding Author

*Phone 734-615-4860; e-mail: scavia@umich.edu.

Notes

The authors declare no competing financial interest.

ACKNOWLEDGMENTS

This work was supported in part by the U.S. EPA STAR Fellowship program, NOAA's Center for Sponsored Coastal Ocean Research grant NA09NOS780204, and the University of Michigan Graham Sustainability Institute. This is NGOMEX contribution 180. This article is Contribution 1776 of the U.S. Geological Survey Great Lakes Science Center. Any use of trade, product, or firm names is for descriptive purposes only and does not imply endorsement by the U.S. Government.

REFERENCES

(1) Rabalais, N. N.; Turner, R. E.; Wiseman, W. J. Gulf of Mexico hypoxia, aka "The dead zone". *Annu. Rev. Ecol. Syst.* **2002**, *33*, 235−263.

(2) LUMCON Hypoxia in the Northern Gulf of Mexico: Research. http://www.gulfhypoxia.net/Research/. (accessed October, 2012.)

(3) Rabalais, N. N.; Turner, R. E.; Scavia, D. Beyond science into policy: Gulf of Mexico hypoxia and the Mississippi River. *Bioscience* **2002**, *52* (2), 129−142.

(4) Rabalais, N. N.; Diaz, R. J.; Levin, L. A.; Turner, R. E.; Gilbert, D.; Zhang, J. Dynamics and distribution of natural and human-caused hypoxia. *Biogeosciences* **2010**, *7* (2), 585−619.

(5) Rabalais, N. N.; Turner, R. E. *Coastal Hypoxia: Consequences for Living Resources and Ecosystems*, Coastal and estuarine studies 58; American Geophysical Union: Washington, D.C., 2001.

(6) *Mississippi River/Gulf of Mexico Watershed Nutrient Task Force Action Plan for Reducing, Mitigating, and Controlling Hypoxia in the Northern Gulf of Mexico*; Office of Wetlands, Oceans, and Watersheds,U.S. Environmental Protection Agency: Washington, DC, 2001; http://water.epa.gov/type/watersheds/named/msbasin/history.cfm.

(7) *Mississippi River/Gulf of Mexico Watershed Nutrient Task Force Gulf Hypoxia Action Plan 2008 for Reducing Mitigating, and Controlling Hypoxia in the Northern Gulf of Mexico and Improving Water Quality in the Mississippi River Basin*; U.S. Environmental Protection Agency, Office of Wetlands, Oceans, and Watersheds: Washington, DC, 2008; http://water.epa.gov/type/watersheds/named/msbasin/actionplan.cfm.

(8) *Hypoxia in the Northern Gulf of Mexico, An Update by the EPA Science Advisory Board*, EPA-SAB-08-003; USEPA: Washington, DC, 2007.

(9) Obenour, D. R.; Michalak, A. M.; Zhou, Y.; Scavia, D. Quantifying the impacts of stratification and nutrient loading on hypoxia in the northern Gulf of Mexico. *Environ. Sci. Technol.* **2012**, *46* (10), 5489−96.

(10) Turner, R. E.; Rabalais, N. N.; Justic, D. Predicting summer hypoxia in the northern Gulf of Mexico: Riverine N, P, and Si loading. *Mar. Pollut. Bull.* **2006**, *52* (2), 139−148.

(11) Turner, R. E.; Rabalais, N. N.; Justic, D. Predicting summer hypoxia in the northern Gulf of Mexico: Redux. *Mar. Pollut. Bull.* **2012**, *64* (2), 319−324.

(12) Forrest, D. R.; Hetland, R. D.; DiMarco, S. F. Multivariable statistical regression models of the areal extent of hypoxia over the Texas-Louisiana continental shelf. *Environ. Res. Lett.* **2011**, *6* (4).

(13) Greene, R. M.; Lehrter, J. C.; Hagy, J. D. Multiple regression models for hindcasting and forecasting midsummer hypoxia in the Gulf of Mexico. *Ecol. Appl.* **2009**, *19* (5), 1161−1175.

(14) Hetland, R. D.; DiMarco, S. F. How does the character of oxygen demand control the structure of hypoxia on the Texas-Louisiana continental shelf? *J. Mar. Syst.* **2008**, *70* (1−2), 49−62.

(15) Fennel, K.; Hetland, D. R.; Feng, Y.; DiMarco, S. F. A coupled physical-biological model of the Northern Gulf of Mexico shelf: Model description, validation and analysis of phytoplankton variability. *Biogeosciences* **2011**, *8*, 1811−1899.

(16) DiMarco, S. F.; Chapman, P.; Walker, N.; Hetland, R. D. Does local topography control hypoxia on the eastern Texas−Louisiana shelf? *J. Mar. Syst.* **2010**, *80*, 25−35.

(17) Scavia, D.; Rabalais, N. N.; Turner, R. E.; Justic, D.; Wiseman, W. J. Predicting the response of Gulf of Mexico hypoxia to variations in Mississippi River nitrogen load. *Limnol. Oceanogr.* **2003**, *48* (3), 951−956.

(18) Scavia, D.; Justic, D.; Bierman, V. J., Jr. Reducing hypoxia in the Gulf of Mexico: Advice from three models. *Estuaries* **2004**, *27* (3), 419−425.

(19) Scavia, D.; Donnelly., K. A. Reassesing hypoxia forecasts for the Gulf of Mexico. *Environ. Sci. Technol.* **2007**, *41*, 8111−8117.

(20) Evans, M. A.; Scavia, D. Forecasting hypoxia in the Chesapeake Bay and Gulf of Mexico: Model accuracy, precision, and sensitivity to ecosystem change. *Environ. Res. Letters* **2010**, DOI: 10.1088/1748-9326/6/1/015001.

(21) Liu, Y.; Evans, M. A.; Scavia, D. Gulf of Mexico hypoxia: Exploring increasing sensitivity to nitrogen loads. *Environ. Sci. Technol.* **2010**, *44* (15), 5836−5841.

(22) Turner, R. E.; Rabalais, N. N.; Justic, D. Gulf of Mexico hypoxia: Alternate states and a legacy. *Environ. Sci. Technol.* **2008**, *42* (7), 2323−2327.

(23) Obenour, D. R. Scavia, D.; Rabalais, N. N.; Turner, R. E.; Michalak, A. M.; A retrospective analysis of mid-summer hypoxic area and volume in the northern Gulf of Mexico, 1985−2011 *Environ. Sci. Technol.* **2013** DOI: 10.1021/es400983g.

(24) http://toxics.usgs.gov/hypoxia/mississippi/flux_ests/delivery/index.html.

(25) Donner, S. D.; Scavia., D. How climate controls the flux of nitrogen by the Mississippi River and the development of hypoxia in the Gulf ofÂ Mexico. *Limnol. Oceanogr.* **2007**, *52* (2), 856−861.

(26) Dinnel, S. P.; Wiseman, W. J., Jr. Fresh water on the Louisiana and Texas shelf. *Cont. Shelf Res.* **1986**, *6*, 765−784.

(27) Gelman, A., J. Hill. *Data Analysis Using Regression and Multilevel/Hierarchical Models*; Cambridge University Press: New York, 2007.

(28) Justić, D.; Rabalais, N. N.; Turner, R. E. Modeling the impacts of decadal changes in riverine nutrient fluxes on coastal eutrophication near the Mississippi River Delta. *Ecol. Modell.* **2002**, *152*, 22−46.

(29) Gronewold, A. D.; Qian, S. S.; Wolpert, R. L.; Reckhow, K. H. Calibrating and validating bacterial water quality models: A Bayesian approach. *Water Res.* **2009**, *43*, 2688−2698.

(30) NOAA National Data Buoy Center (NDBC); http://www.ndbc.noaa.gov/ (accessed July, 2012.)

(31) Murrell, M. C.; Stanley, R. S.; Lehrter, J. C.; Hagy, J. D., III Plankton community respiration, net ecosystem metabolism, and oxygen dynamics on the Louisiana continental shelf, Implications for hypoxia. *Cont. Shelf Res.* **2013**, *52*, 27−38.

(32) McCarthy, M. J.; Carini, S. A.; Liu, Z.; Ostrom, N. E.; Gardner, W. S. Oxygen consumption in the water column and sediments of the northern Gulf of Mexico hypoxic zone. *Estuarine, Coastal Shelf Sci.* **2013**, *123*, 46−53.

(33) Sprague, L. A.; Hirsch, R. M.; Aulenbach, B. T. Nitrate in the Mississippi River and it tributaries, 1980−2007: Are we making progress? *Environ. Sci. Technol.* **2011**, *45*, 7209−7216.

(34) Scavia, D.; Kelly, E. A.; Hagy, J. D., III. A simple model for forecasting the effects of nitrogen loads on Chesapeake Bay hypoxia. *Estuaries Coasts* **2006**, *29* (4), 674−684.

(35) Stow, C. A.; Scavia, D. Modeling Hypoxia in the Chesapeake Bay: Ensemble Estimation Using a Bayesian Hierarchical Model. *J. Mar. Syst.* **2009**, *76*, 244−250.